Inorganic Chemistry

Article

pubs.acs.org/IC

The Intramolecular Rearrangement of Phosphinohydrazides [R′$_2$P−NR−NR−M] → [RN═PR′$_2$−NR−M]: General Rules and Exceptions. Transformations of Bulky Phosphinohydrazines (R−NH−N(PPh$_2$)$_2$, R = *t*Bu, Ph$_2$P)

Alexander N. Kornev,*[,†] Vyacheslav V. Sushev,[†] Yulia S. Panova,[†] Natalia V. Belina,[†] Olga V. Lukoyanova,[†] Georgy K. Fukin,[†] Sergey Y. Ketkov,[†] Gleb A. Abakumov,[†] Peter Lönnecke,[‡] and Evamarie Hey-Hawkins[‡]

[†]Razuvaev Institute of Organometallic Chemistry, Russian Academy of Sciences, 49 Tropinin Street, 603950 Nizhny Novgorod, Russia

[‡]Institut für Anorganische Chemie, Universität Leipzig, Johannisallee 29, D-04103 Leipzig, Germany

Supporting Information

ABSTRACT: Reactions of diphosphinohydrazines R−NH−N(PPh$_2$)$_2$ (R = *t*Bu (**1**), Ph$_2$P (**3**)) with some metalation reagents (Co[N(SiMe$_3$)$_2$]$_2$, LiN(SiMe$_3$)$_2$, La[N(SiMe$_3$)$_2$]$_3$, *n*BuLi, MeLi) were performed. Compound **1** was synthesized by the reaction of Ph$_2$PCl with *tert*-butylhydrazine hydrochloride in 83% yield. This compound reveals temperature-dependent ^{31}P NMR spectra due to hindered rotation about the P−N bonds. Complicated redox reaction of **1** with Co[N(SiMe$_3$)$_2$]$_2$ proceeds with cleavage of the P−N and N−N bonds to form a binuclear cobalt complex [Co{HN(PPh$_2$)$_2$-κ^2P,P′}$_2$(μ-PPh$_2$)]$_2$ (**2**) demonstrating a short Co···Co distance of 2.3857(5) Å, which implies a formal double bond between the Co atoms. Strong nucleophiles (*n*BuLi, MeLi) cause fragmentation of the molecules **1** and **3**, while reactions of **3** with lithium and lanthanum silylamides give products of the NNP → NPN rearrangement [Li{Ph$_2$P(NPPh$_2$)$_2$-κ^2N,N′}(THF)$_2$] (**4**) and [La{Ph$_2$P(NPPh$_2$)$_2$-κ^2N,N′}{N(SiMe$_3$)$_2$}$_2$] (**5**), respectively. These complexes represent the first examples of a κ^2N,N′ bonding mode for the triphosphazenide ligand [(Ph$_2$PN)$_2$PPh$_2$]$^-$. DFT calculations showed large energy gain (52.1 kcal/mol) of the [NNP]$^-$ to [NPN]$^-$ anion rearrangement.

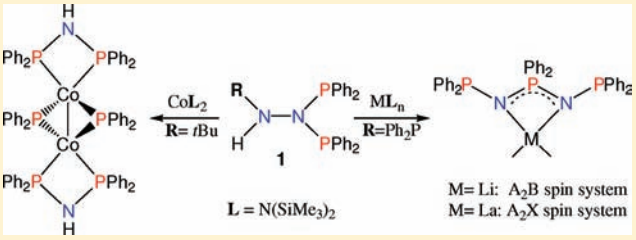

INTRODUCTION

Heteroatom ligands containing a phosphorus(III)−nitrogen bond have many applications in organometallic chemistry and catalysis. Important examples are catalytic C−H bond activation,[1] hydroformylation of alkenes to give commercially valuable alcohols instead of aldehydes,[2] palladium catalyzed Heck, Suzuki, and amination reactions of aryl chlorides.[3] The chemistry of phosphinoamides has lately received considerable attention because of two possible resonance structures, [R′$_2$PNR]− and [R′$_2$P═NR]. These heterofunctional systems often display unique dynamic features, such as hemilability, which provides an efficient molecular activation procedure under mild conditions that is very important for catalytic applications.[4] Simple phosphinoamides (R$_2$P−NR′−) may be synthesized very easily by the direct interaction of chlorophosphines with secondary amines.[5,6] The approaches to the oligophosphazenides with R$_2$P(III)-terminal groups are not so easy. As an example, it is known that the triphosphazenide ligand [Ph$_2$P−N═PPh$_2$−NPPh$_2$]$^-$ may be synthesized only in the coordination sphere of transition metals by the disproportionation of bis(diphenylphosphino)amide anion.[7−9] So, cobalt(II) chloride and LiN(PPh$_2$)$_2$ in boiling toluene form a triphosphazenide anion by oxidative scrambling of the amide, which reacts further with cobalt(II) to give the spirocyclic metallaphosphazene.[8] During our study we described the rearrangement of phosphinohydrazides,[10−15] which may be considered as a useful approach to the synthesis of phosphazenides and phosphinoamides (Scheme 1).

Like the Michaelis−Arbuzov rearrangement[16] and its modifications involving transition-metal centers,[17] the major driving force of these reactions is the formation of tetracoordinated phosphorus(V) species instead of phosphorus(III). Meanwhile, there are a number of examples for complexes in which the rearrangement of phosphinohydrazides does not occur: (Ge(NPh−NPh−PPh$_2$)$_2$;[10] Co(NPh−NPh−P(*i*Pr)$_2$ and Ni(NPh−NPh−P(*i*Pr)$_2$).[13] The tendency of the phosphinohydrazide system toward rearrangement depends on several factors. These are the energies of the covalent N−N and coordination M−P bonds that ought to be cleaved in the course of the reaction. We have shown[13,15] that the main factor, which controls the P−N−N to N═P−N rearrangement, is the charge

Received: July 27, 2011
Published: December 30, 2011

Scheme 1. Rearrangements of Mono-, Bis-, and Trisphosphinohydrazides[a]

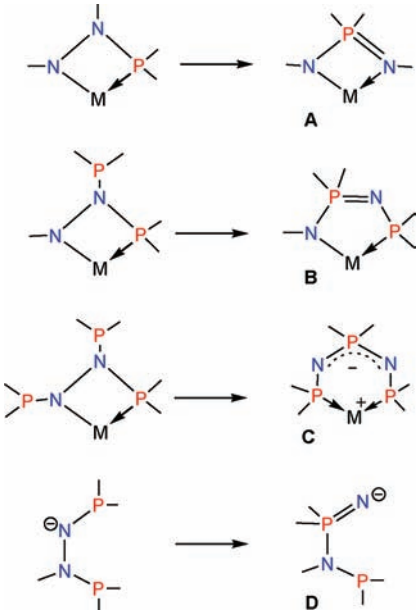

[a]M = metal atom.

at the hydrazido nitrogen. A strong negative charge promotes elongation of the N–N bond and its cleavage in the first step of the reaction. Tentatively, the rearrangement proceeds via several intermediate steps, depicted in the Schemes 2 and 3.

Scheme 2. Proposed Mechanism for the Rearrangement of Monophosphinohydrazides

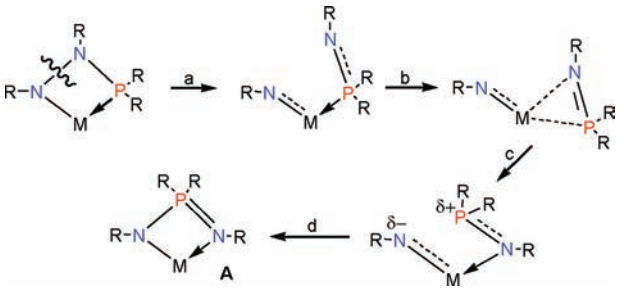

Scheme 3. Proposed Mechanism for the Rearrangement of Diphosphinohydrazides

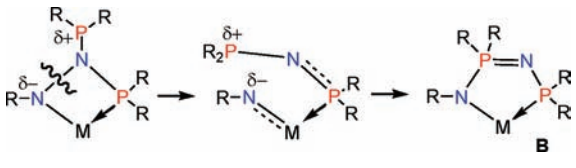

The product **A** (Scheme 2), having a single phosphorus(V) atom, can be formed only after cleavage of the P→M coordination bond. Cleavage of the P→M bond is not necessary for the formation of **B**, having two phosphorus atoms (Scheme 3). Both schemes include formation of a novel P–N bond by the interaction of positively charged phosphorus and negatively charged nitrogen atoms. According to these schemes, electron-withdrawing substituents at phosphorus and electron-donating groups at nitrogen will favor the rearrangement. On the other hand, it is reasonable to propose that the possibility of the P–N bond formation depends on the steric properties of the substituents at nitrogen and phosphorus. In order to check this assumption we have explored transformations of phosphinohydrazines R–NH–N(PPh_2)$_2$ bearing bulky substituents (R = *t*Bu, Ph_2P) upon metalation. Note that the steric effect of the Ph_2P group in phosphinoamides[18] can vary considerably (unlike *t*Bu) since the P–N bond length is strongly dependent on the charge localized on the phosphinoamide group, so that a formal P–N single bond demonstrates more π-type character in phosphinoamides.[19]

For metalation of phosphinohydrazines we used cobalt silylamide, Co[N($SiMe_3$)$_2$]$_2$ (the model reagent for a number experiments), and some nucleophiles {LiN($SiMe_3$)$_2$, La[N($SiMe_3$)$_2$]$_3$, *n*BuLi, MeLi}, containing strongly coordinating hard metal cations.

RESULTS AND DISCUSSION

1-*tert*-Butyl-2-bis(diphenylphosphino)hydrazine (**1**) was prepared in 83% yield as colorless crystals by the reaction of *tert*-butylhydrazine hydrochloride with 2 equiv of Ph_2PCl in THF:

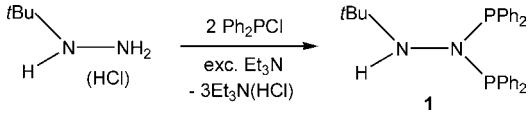

In the solid state compound **1** exists as a mixture of stereoisomers **1a,b** (two crystallographic independent molecules) that differ in the orientation of the *tert*-butyl group with respect to the unsymmetrical NP_2 fragment:

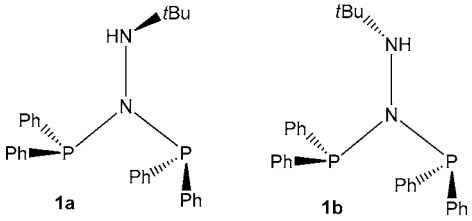

Both stereoisomers have very similar structural parameters. The molecular structure of **1a** is shown in Figure 1 with selected bond lengths and angles. The crystallographic data and the details of the structure determination are given in Table 1. The corresponding data for **1b** are given in Figure S1 and Table S1 in the Supporting Information.

Formation of stereoisomers is possible due to hindered rotation around the P–N and N–N bonds. The molecule has a nearly planar P_2NN core. The sum of bond angles at N(1) is 357.6°. Steric demand of the *tert*-butyl group results in elongation of the N–N bond (1.445(1) Å) as compared to the known phosphinohydrazines (1.401(2) Å in Ph_2P–NPh–NPh–H,[10] 1.418(1) in 8-quinolyl-NH–N(PPh_2)$_2$).[15] This value is very close to that found in the other sterically hindered hydrazine (Ph_2P)$_2$N–NH–PPh_2 (1.437(3) Å).[12] There is a variation between P–N bond lengths in the crystal structure of **1** (1.718(1) Å and 1.729(1) Å in **1a**; 1.731(1) Å and 1.719(1) Å in **1b**). In general, the P–N bond lengths and P–N–P bond angles (120.38(6)° and 118.86(6)° for **1a** and **1b** respectively) are typical for this kind of ligand.[20]

The ^{31}P NMR spectrum of **1** reveals a broad singlet (δ 71.0 ppm) at ambient temperatures, but forms two spin-coupled doublets (AB spin system) at 193 K (Figure 2).

The signals for the two Ph_2P groups at 76.0 and 67.5 ppm coalesced at 273 K. Changes in the multiplicity of the ^{31}P

dx.doi.org/10.1021/ic201617p | Inorg. Chem. 2012, 51, 874–881

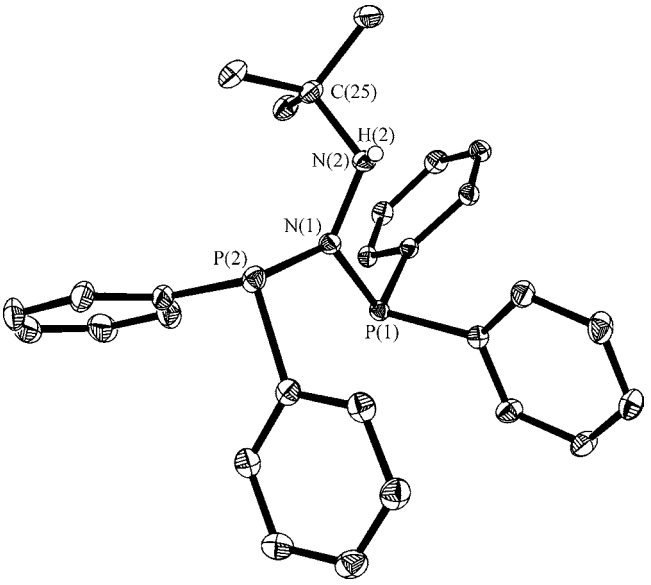

Figure 1. The molecular structure of **1a** with ellipsoids of 30% probability. Hydrogen atoms except H(2) were omitted for clarity. Selected bond lengths (Å) and angles (deg) for **1**: P(1)–N(1) 1.718(1), P(2)–N(1) 1.729(1), N(1)–N(2) 1.445(1), N(2)–C(25) 1.494(2), N(2)–H(2) 0.89(2); N(2)–N(1)–P(1) 118.9(1), N(2)–N(1)–P(2) 118.3(1), P(1)–N(1)–P(2) 120.4(1), N(1)–N(2)–C(25) 116.6(1), N(1)–N(2)–H(2) 106(1).

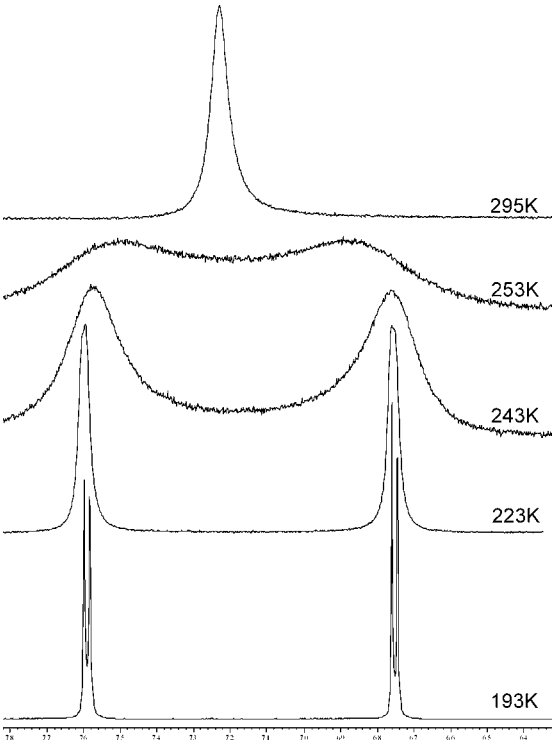

Figure 2. Series of variable-temperature ^{31}P NMR spectra for **1**.

signals can be interpreted in terms of restricted rotation about the P–N bonds. The activation energy of the dynamic process was found to be 10.9 kcal mol^{-1}. The appearance of two spin-coupled doublets at low temperatures indicates the presence of conformers with C_s symmetry in solution. The observed coupling constant ($J_{P,P}$ = 25 Hz) and general appearance of the variable-temperature ^{31}P NMR spectra for **1** are very similar to those reported for bis(diphenylphosphino)amines R–N-$(PPh_2)_2$ (R = *i*Pr,[20] CHMePh).[21]

Earlier we have reported reactions between a similar ligand, $(Ph_2P)_2N$–NH–Ph, and transition metal silylamides Co[N-$(SiMe_3)_2]_2$ and $[NiN(SiMe_3)_2(PPh_3)_2]$, which result in

Table 1. Crystal and Structure Refinement

	1	2	4	5
empirical formula	$C_{28}H_{30}N_2P_2$	$C_{80}H_{78}Co_2N_2O_2P_6$	$C_{44}H_{46}LiN_2O_2P_3$	$C_{48}H_{66}LaN_4P_3Si_4$
formula wt	456.48	1403.12	734.68	1043.23
temp, K	130(2)	100(2)	150(2)	100(2)
cryst syst	monoclinic	monoclinic	monoclinic	triclinic
space group	$P2_1/c$	$P2_1/n$	$P2_1/c$	$P\bar{1}$
a, Å	12.3019(1)	16.1309(8)	10.0645(3)	11.5932(4)
b, Å	31.7222(3)	21.1279(10)	25.9844(9)	12.2192(4)
c, Å	12.9120(2)	19.9712(9)	15.3793(5)	20.8318(6)
α, deg	90	90	90	86.390(1)
β, deg	90.004(1)	94.437(1)	101.985(1)	84.327(1)
γ, deg	90	90	90	63.190(1)
vol, Å^{-3}	5038.8(1)	6786.0(6)	3934.3(2)	2620.4(2)
Z	8	4	4	2
cryst size, mm^3	0.53 × 0.39 × 0.28	0.30 × 0.15 × 0.08	0.35 × 0.35 × 0.35	0.25 × 0.23 × 0.15
abs coeff, mm^{-1}	0.191	0.681	0.190	1.034
abs correction	SCALE3 ABSPACK	SADABS	SADABS	SADABS
max./min transmission		0.9475/0.8218	0.9364/0.9364	0.8604/0.7822
density (calcd), Mg/m^3	1.203	1.373	1.240	1.322
reflns collected	120353	57210	23285	25274
indep reflns	15400 [*R*(int) = 0.0429]	13284 [*R*(int) = 0.1296]	7728 [*R*(int) = 0.0281]	11901 [*R*(int) = 0.0204]
data/restraints/params	15400/0/818	13284/26/847	7728/0/469	11901/9/757
R indices [$I > 2\sigma(I)$]	R1 = 0.0391, wR2 = 0.0869	R1 = 0.0595, wR2 = 0.0956	R1 = 0.0519, wR2 = 0.1433	R1 = 0.0305, wR2 = 0.0718
R indices (all data)	R1 = 0.0489, wR2 = 0.0915	R1 = 0.1202, wR2 = 0.1075	R1 = 0.0693, wR2 = 0.1540	R1 = 0.0374, wR2 = 0.0745
largest diff. peak and hole, e·Å^{-3}	0.310 and −0.259	0.664 and −0.513	1.045 and −0.340	1.149 and −0.444
GOF	1.19	0.998	1.067	1.059

dx.doi.org/10.1021/ic201617p | *Inorg. Chem.* 2012, 51, 874–881

formation of spirocyclic complexes [M{NPh−PPh_2=N−PPh_2}$_2$] (M = Co, Ni), demonstrating a rearrangement of the ligand.[11] Following these observations, we have explored ligand **1** containing the bulkier *t*Bu group at nitrogen in the reaction with cobalt(II) bis(trimethylsilyl)amide. The reaction proceeds at room temperature in toluene solution for 48 h to give the only isolable product **2** as red-brown crystals:

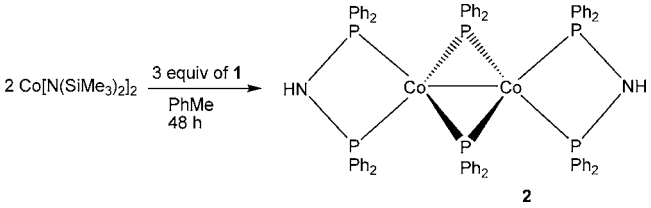

The molecular structure of **2** is shown in Figure 3 with selected bond lengths and angles.

Each Co atom in the dimeric molecule is coordinated by one bis(diphenylphosphino)amine ligand (DPPA) and two bridging PPh_2 groups. The $Co_2(\mu\text{-P})_2$ core is rigorously planar; notable are the acute Co(1)−P(3)−Co(2) and Co(1)−P(4)−Co(2) bond angles of 66.56(2)° and 66.04(2)°, respectively. Both P(1)Co(1)P(2) and P(5)Co(2)P(6) planes form dihedral angles with the $Co_2(\mu\text{-P})_2$ core of 67.3° and 76.1°, respectively. The Co−Co distance in **2** (2.3857(5) Å) is much shorter than the sum of the covalent radii (2.52 Å),[22] which implies a formal double bond between the Co atoms, as required to achieve 18 valence electrons about each metal. For comparison, a nonbonding Co···Co distance of 3.573(2) Å found in $[Co_2\{\mu\text{-}PPh_2\}_2(CO)_6]$,[23] a single Co−Co bond of 2.56(1) Å in $[(CpCo)_2\{\mu\text{-}PPh_2\}_2]$[24] and a double bond of 2.343(2) Å in $[Co_2\{\mu\text{-}PPh_2\}_2(CO)_2(PEtPh)_2]$[25] are in agreement with our data. The unit cell contains two THF molecules per one molecule of **2**, which form hydrogen bonds with NH group of both DPPA ligands (Figure S2 in the Supporting Information).

Computational optimization of the molecular structure of **2** at the B3LYP/6-31G(d) level of theory also resulted in a short Co−Co distance (2.310 Å) (Figure S3 in the Supporting Information). Molecular orbitals for **2** are presented in Figure 4. NBO analysis reveals that the metal−metal bond is formed mainly by the 3d and 4p electrons of cobalt. An MO isosurface study shows that the HOMO corresponds to the π-type Co−Co wave function overlapping while HOMO−1 and HOMO−7 are responsible for the σ- and δ-bonding, respectively (Figure 5).

Additional evidence for the existence of a direct metal−metal bond in **2** is provided by analysis of the electron density topology performed within Bader's AIM theory.[26] Our AIM study reveals a Co−Co (3,−1) critical point corresponding to the chemical bond (Figure S4 in the Supporting Information).

It is quite obvious that the reaction of **1** with Co[N-$(SiMe_3)_2]_2$ proceeds with N−N and P−N bond cleavage caused by the presence of the *t*Bu group. We have no intention to study the mechanistic aspects of this transformation in detail, but some tentative conclusions are given here. The first step of the reaction, undoubtedly, is coordination of **1** to the cobalt atom via the Ph_2P group. The NH proton is unlikely to be abstracted by the $(Me_3Si)_2N$ group due to steric reasons. Instead, formation of tetrakis(trimethylsilyl)hydrazine was registered by GLC. This is in agreement with the redox scheme of the reaction, since no compounds with cobalt in high oxidation states (namely, Co^{3+}) were found in the reaction mixture. Liberation of $(Me_3Si)_2NN(SiMe_3)_2$ is known to proceed in some reactions of transition metal silylamides.[27,28] It may be supposed also that the formation of the spirocyclic complex [Co{N**R**−PPh_2=N−PPh_2}$_2$] (R = *t*Bu) is not easy because of steric hindrance as compared to related compounds {M{N**R**−PPh_2=N−PPh_2}$_2$] (R = Ph, M = Co, Ni).[11] Instead, fragmentation of the molecule is observed.

Interestingly, the lithium salt of **1** was not obtained at ambient conditions while many other lithium phosphinohydrazides were characterized in crystalline form or in solution.[10−15] Thus, unexpectedly the reaction between **1** and MeLi in toluene/Et_2O solution gave a mixture of products, $LiPPh_2$, Ph_2P−PPh_2, Ph_2PMe and *t*Bu−PPh_2 according to the ^{31}P NMR spectra and chromatography−mass spectrometry measurements (Supporting Information, page 8). Interaction of **1** with *n*-BuLi proceeds in a similar way to give Ph_4P_2 and

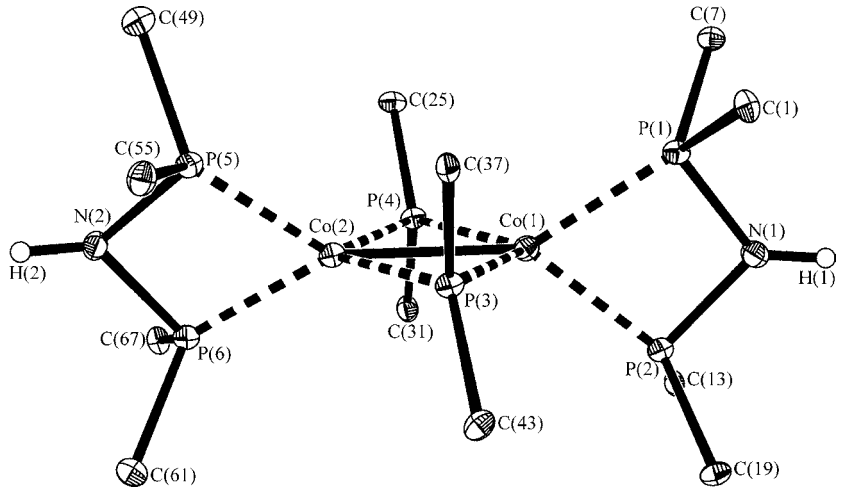

Figure 3. The molecular structure of **2** with ellipsoids of 30% probability. Phenyl groups were omitted for clarity. Selected bond lengths (Å) and angles (deg) for **2**: Co(1)−Co(2) 2.3857(5), Co(1)−P(3) 2.1671(8), Co(1)−P(1) 2.1750(8), Co(1)−P(4) 2.1878(8), Co(1)−P(2) 2.1896(8), P(1)−N(1) 1.687(2); P(3)−Co(1)−P(4) 114.00(3), P(1)−Co(1)−P(2) 72.52(3), P(6)−Co(2)−P(5) 72.45(3), P(3)−Co(2)−P(4) 113.36(3), P(4)−Co(1)−P(2) 115.06(3), N(1)−P(1)−Co(1) 93.93(8), N(1)−P(2)−Co(1) 93.52(8), Co(1)−P(4)−Co(2) 66.04(2), P(1)−N(1)−P(2) 100.0(1), P(5)−N(2)−P(6) 97.9(1).

dx.doi.org/10.1021/ic201617p | *Inorg. Chem.* 2012, 51, 874−881

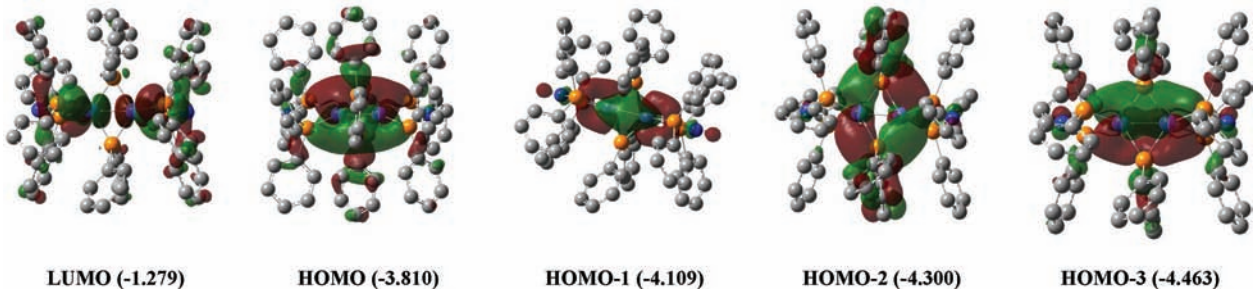

Figure 4. Molecular orbitals for **2** and their energies in electronvolts are provided.

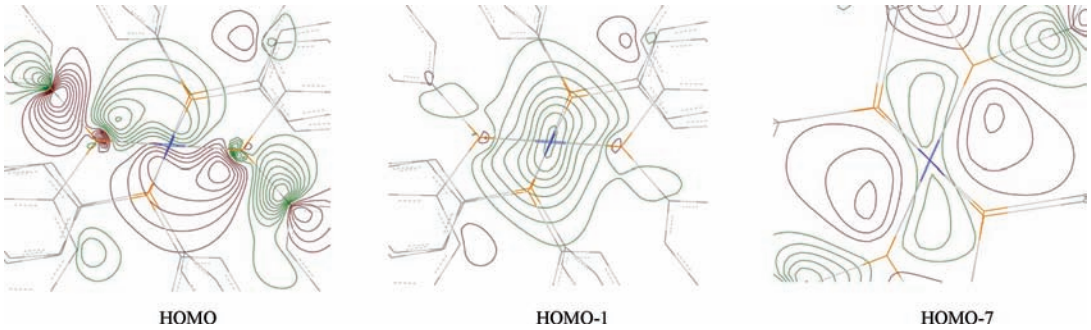

Figure 5. Contour maps for the HOMO, HOMO−1 and HOMO−7 of the **2** molecule in the plane orthogonal to the Co−Co bond and bearing two bridging P atoms. The contours start at 0.01/−0.01 E_h, and the step is 0.01/−0.01 E_h.

$LiPPh_2$ as the main products. At the same time, more sterically hindered $LiN(SiMe_3)_2$ does not react with **1** at all. Thus, the behavior of **1**, containing a bulky *t*Bu group, in metalation reactions is quite different from that of known phosphinohydrazines.[10−15]

In view of these results, the behavior of the related ligand, tris(diphenylphosphino)hydrazine (**3**) (R = Ph_2P), deserves detailed consideration. Earlier we have reported the reactions of **3** with $Co[N(SiMe_3)_2]_2$ and $NiCp_2$ which gave six-membered cyclic metallophosphazenes[12] as a result of the rearrangement

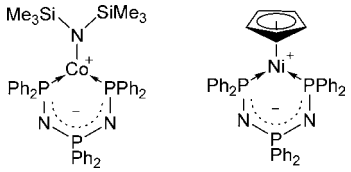

of this ligand in the coordination sphere of cobalt(II) and nickel(II):

Meanwhile, our attempts to synthesize the lithium salt of **3** or its rearrangement product by reaction with *n*BuLi were unsuccessful.[12] Instead, a complex mixture of products was formed. Among them $(Ph_2P)_2NH$ (^{31}P NMR δ 44.5 ppm) was found, which is indicative of the N−N bond cleavage in **3**. More importantly, lithium silylamide, $LiN(SiMe_3)_2$, reacts with **3** to form the rearrangement product **4** only in 78% yield:

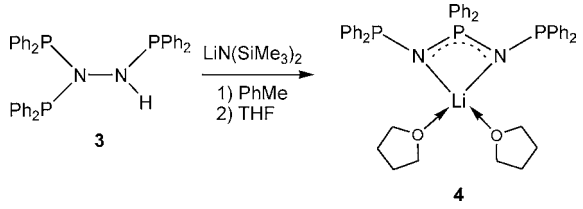

3 **4**

The reaction proceeds in toluene solution at ambient conditions; the product was crystallized by addition of THF and cooling to 0 °C. The molecular structure of **4** with selected bond lengths and angles is shown in Figure 6. The crystallographic data and details of the structure determination are given in Table 1.

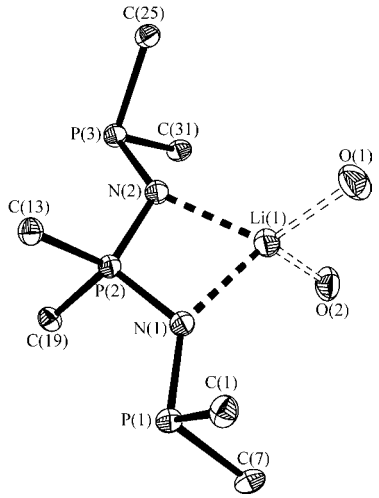

Figure 6. The molecular structure of **4** with ellipsoids of 30% probability. Phenyl groups, atoms C of the THF molecule and hydrogen atoms were omitted for clarity. Selected bond lengths (Å) and angles (deg) for **4**: P(1)−N(1) 1.673(1), P(2)−N(2) 1.601(1), P(2)−N(1) 1.601(1), P(3)−N(2) 1.680(1), Li(1)−N(2) 2.061(3), Li(1)−N(1) 2.067(3), Li(1)−O(2S) 1.918(3,) Li(1)−O(1S) 1.955(3); O(2S)−Li(1)−O(1S) 100.1(2), N(2)−Li(1)−N(1) 75.4(1), N(2)−P(2)−N(1) 104.10(7), P(2)−N(1)−P(1) 125.44(9), P(2)−N(1)−Li(1) 90.1(1), P(2)−N(2)−P(3) 122.80(9), P(2)−N(2)−Li(1) 90.3(1).

dx.doi.org/10.1021/ic201617p | *Inorg. Chem.* 2012, 51, 874−881

The open PNPNP phosphazenide chain in **4** is coordinated to the lithium atom by two nitrogen atoms to form an entirely planar four-membered metallacycle. The geometry about the lithium atom (additionally coordinated by two THF molecules) is distorted tetrahedral with O(2S)–Li(1)–O(1S) and N(2)–Li(1)–N(1) angles of 100.1(2)° and 75.4(1)°, respectively.

The terminal P–N bonds, P(1)–N(1) of 1.673(1) Å and P(3)–N(2) of 1.680(1) Å, which exert single-bond character are longer than the internal P–N bonds P(2)–N(2) of 1.601(1) Å and P(2)–N(1) of 1.601(1) Å, that participate in the delocalized bonding scheme.

It is well-known that the ligand $[Ph_2PNP(Ph_2)NPPh_2]$ forms six-membered metallacycles with transition metals (Co, Ni,[7,8,12] Fe[9]) by κ^2P,P′-complexation. To the best of our knowledge, compound **4** is the first example of a κ^2N,N′ bonding mode for this ligand.

Bearing in mind the differences between the reagents *n*BuLi and $LiN(SiMe_3)_2$ in the reaction with **3**, we have explored related reactions of **3** with lanthanum and sodium silylamides.

As expected, both silylamides react with **3**, but lanthanum silylamide, $La[N(SiMe_3)_2]_3$, reacts very cleanly. The reaction proceeds in toluene solution at 115 °C in 5 h with substitution of one $(Me_3Si)_2N$ group to give **5** in 92% yield. Using an excess of **3** in the reaction does not result in substitution of a second silylamide group. Apparently, the formation of the tight chelate increases the strength of the remaining La–$N(SiMe_3)_2$ bonds. Steric hindrances also should be taking into consideration.

Note that at room temperature the process was not observed; on the other hand, at temperatures above 130 °C the starting material converts into another products, $(Ph_2P)_2NH$ and $(Ph_2PN)_4$, as we have described earlier.[12]

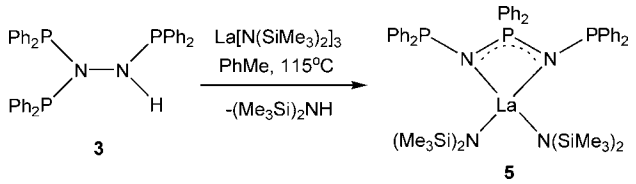

3 **5**

The molecular structure of **5** with selected bond lengths and angles is shown in Figure 7. The crystallographic data and details of the structure determination are given in Table 1.

Similar to the lithium salt **4**, the PNPNP phosphazenide chain in **5** is coordinated to lanthanum via two nitrogen atoms to form a nearly planar four-membered metallacycle. The geometry about the lanthanum atom (additionally coordinated by two $(Me_3Si)_2N$ ligands) is distorted tetrahedral with N(1)–La(1)–N(2) and N(3)–La(1)–N(4) bond angles of 60.00(4)° and 116.58(5)°, respectively. The terminal P–N bonds of 1.725(1) and 1.717(1) Å indicate single-bond character, while the shorter internal P–N bonds of 1.623(1) and 1.624(1) Å participate in the delocalized bonding scheme. The P–N bond lengths in **4** and **5** are represented for comparison in a single scheme:

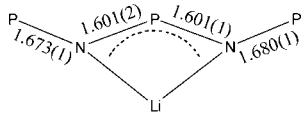

4

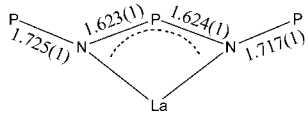

5

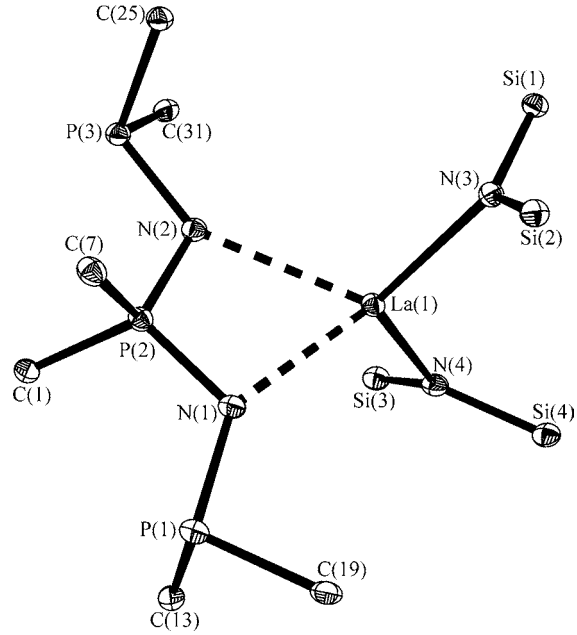

Figure 7. The molecular structure of **5** with ellipsoids of 30% probability. Phenyl and methyl groups and hydrogen atoms were omitted for clarity. Selected bond lengths (Å) and angles (deg) for **5**: La(1)–N(3) 2.374(1), La(1)–N(4) 2.377(1), La(1)–N(1) 2.518(1), La(1)–N(2) 2.583(1), P(2)–N(1) 1.623(1), P(2)–N(2) 1.624(1), P(1)–N(1) 1.725(1), P(3)–N(2) 1.717(1); N(3)–La(1)–N(4) 116.58(5), N(1)–La(1)–N(2) 60.00(4), N(1)–P(2)–N(2) 103.59(7), P(1)–N(1)–P(2) 115.83(8), P(2)–N(2)–P(3) 116.24(8).

It is surprising to see that the P–N bonds in the lanthanum complex are notably longer than the corresponding P–N bonds in the lithium derivative. This difference may reflect the greater steric bulk of the molecule **5** due to the presence of $(Me_3Si)_2N$ group. Note that the known six-membered metallacycles with a $[(Ph_2PN)_2PPh_2$-κ^2P,P′$]^-$ ligand exhibit averaged N–P bond lengths (1.59–1.62 Å).[7,9,12]

Since complexes **4** and **5** have notably different P–N bond lengths, the corresponding $J_{P,P}$ coupling constants in the ^{31}P NMR spectra are expected to be rather different. The proton-decoupled ^{31}P NMR spectrum of the lanthanum complex **5** (A_2X spin system) consists of a doublet (δ 41.7, $^2J_{P,P}$ = 36 Hz) and a triplet (δ 34.2, $^2J_{P,P}$ = 36 Hz) at room temperature in a ratio of 2:1 (Figure S5 in the Supporting Information). The lithium complex **4** demonstrates similar chemical shifts (δ 42.7 and 34.1 ppm) but a more complex ^{31}P{^{1}H} NMR spectrum, which was assigned to an A_2B spin system with an AB coupling constant of 120 Hz (Figure S6 in the Supporting Information). Apparently, shortening P–N bonds in **4** (as compared to those in **5**) makes s-orbital character on phosphorus atoms more considerable, which determines a larger $^2J_{P,P}$ coupling constant observed for **4**.

We have also explored the similar reaction of **3** with sodium silylamide, $NaN(SiMe_3)_2$, in toluene/THF solution. The ^{31}P NMR spectrum of the reaction mixture showed a broad resonance (a doublet at 42.1, $^2J_{P,P}$ = 98 Hz) and a triplet (δ 34.5, $^2J_{P,P}$ = 98 Hz) at room temperature. Unfortunately, attempts to crystallize the sodium salt only gave a solid of insufficient purity.

DFT calculations showed that a rearrangement of the neutral molecule $(Ph_2P)_2N$–NH–PPh_2 to the iminophosphorane

dx.doi.org/10.1021/ic201617p | *Inorg. Chem.* 2012, 51, 874–881

$Ph_2P-N{=}PPh_2-NH-PPh_2$ is energetically favorable by 31.5 kcal/mol. The total energies of the two isomers were compared without modeling the rearrangement process (Table S2 in the Supporting Information). However, more importantly, the rearrangement of the anion $[(Ph_2P)_2N-N(PPh_2)]^-$ (model compound without metal counterion) to the iminophosphoranate anion $[(Ph_2PN)_2PPh_2]^-$ is a much more favorable process (by 52.1 kcal/mol) (Table S3 in the Supporting Information). The possibility of enhanced charge delocalization in the iminophosphoranate anion as compared to the isomeric phosphinohydrazide (Tables S4–S7 in the Supporting Information) gives an additional ~20 kcal/mol, which makes the NNP → NPN rearrangement extremely favorable.

CONCLUSION

In summary, considering the ligands $R-NH-N(PPh_2)_2$ (R = *t*Bu (**1**), Ph_2P (**3**)) with respect to NNP → NPN rearrangement, the electron-donating, bulky *t*Bu group apparently encourages N–N bond cleavage, but its steric demand may prevent the P–N coupling reaction and rearrangement of the ligand. Instead, fragmentation of the molecule is observed to give $HN(PPh_2)_2$ and diphenylphosphanido fragments as new building blocks as was observed in the binuclear cobalt complex $[Co\{HN(PPh_2)_2\text{-}\kappa^2P,P'\}_2(\mu\text{-}PPh_2)]_2$ (**2**). The phosphinohydrazines **1** and **3** react with *n*BuLi to give decomposition products. More intriguing results were obtained while exploring the reactivity of **3** toward lithium and lanthanum silylamides. Both reactions gave products resulting from rearrangement of phosphinohydrazide to the iminophosphoranate, $[(Ph_2PN)_2PPh_2]^-$, which exhibits κ^2N,N' coordination to the metal (Li or La).

Computation of total energies for the triphosphinohydrazine $Ph_2PNH-N(PPh_2)_2$ and isomeric iminophosphoirane $Ph_2P-N{=}PPh_2-NH-PPh_2$ has shown the energy difference of 31.5 kcal/mol. At the same time, the difference between total energies of hydrazido anion $[Ph_2P-NN(PPh_2)_2]^-$ and isomeric iminophosphoranate $[(Ph_2PN)_2PPh_2]^-$ is significantly higher (ΔE = 52.1 kcal/mol). An additional ~20 kcal/mol comes from the possibility of enhanced charge delocalization in the iminophosphoranate which makes the rearrangement of phosphinohydrazide anion extremely favorable.

EXPERIMENTAL SECTION

General Remarks. Solvents were purified following standard methods.[29] Toluene was thoroughly dried and distilled over sodium metal prior to use. Diethyl ether and THF were dried and distilled over Na/benzophenone. The silylamides $[Co\{N(SiMe_3)_2\}_2]$[30,31] and $[La\{N(SiMe_3)_2\}_3]$[32] were prepared according to known methods. All manipulations were performed with rigorous exclusion of oxygen and moisture, in a vacuum or under an argon atmosphere using standard Schlenk techniques. The spectrophotometric determination of cobalt in **2** was provided by the method described in ref 33. Infrared spectra were recorded on a Bruker spectrometer Vertex 70 from 400 to 4000 cm^{-1} in Nujol mulls on KBr plates. NMR spectra were recorded in $CDCl_3$ or C_6D_6 solutions using a Bruker DPX-200 device. The identity of the reaction products $(Me_3Si)_2NH$ and $(Me_3Si)_2NN(SiMe_3)_2$ was established by comparison of retention times with authentic samples using gas chromatography analyses with a Tsvet-500 device, equipped with 0.4 cm × 200 cm stainless steel columns, packed with 5% SE-30 on Chromatone N-Super, with a thermoconductivity detector and with helium as a carrier gas.

X-ray Crystallography. The X-ray diffraction data were collected on an Xcalibur-S (Agilent Technologies) for **1** and on a SMART APEX diffractometer for **2**, **4**, and **5** (graphite-monochromated, Mo Kα radiation, $\varphi-\omega$-scan technique, λ = 0.71073 Å). All structures were solved by direct methods and were refined on F^2_{hkl} using SHELXL-97 packages.[34] All non-hydrogen atoms in **1**, **2**, **4**, and **5** were refined anisotropically. All H atoms in **1**, H(N) atoms in **2** and all H atoms except methyl hydrogens at C(37), C(40), C(42), C(47) in **5** were found from Fourier syntheses of electron density and were refined isotropically. Other hydrogen atoms in **2**, **4**, and **5** were placed in calculated positions and were refined in the riding model. SCALE3 ABSPACK[35] (for **1**) and SADABS[36] were used to perform absorption corrections in **2**, **4**, and **5**. The crystal for **1** was found to be slightly twinned (twin law by rows, −1 0 0, 0 −1 0, 0 0 1; twin domain ratio 0.947(1), 0.053(1). The main crystallographic data and structure refinement details for **1**, **2**, **4**, and **5** are presented in Table 1.

DFIX Instructions were used for the fix of geometry of THF molecules in **2** and some objectively detected the C–H distances in **5**.

CCDC 819234 (**1**), 819235 (**2**), 819236 (**4**), and 819237 (**5**) contain the supplementary crystallographic data for this paper. These data can be obtained free of charge at www.ccdc.cam.ac.uk/data_request/cif from the Cambridge Crystallographic Data Centre.

Computational Details. DFT calculations performed in this work were carried out at the B3LYP/6-31G(d) level of theory with the Gaussian 03 package (Supporting Information). The optimized geometries of **2** and the anions $[(Ph_2PN)_2PPh_2]^-$ and $[(Ph_2P)_2N-NPPh_2]^-$ correspond to energy minima. Frequency calculations for every mentioned structure were performed. There are no imagery frequencies in every case. For the geometry optimization of **2** we used the full structure without simplification. The NBO analysis[37] was performed to analyze the charge distribution in the molecules investigated. The electron density topology was investigated within the frames of Bader's atom in molecules theory[26] with use of the AIMAll package.[38]

Synthesis. *t*BuN(H)–N(PPh$_2$)$_2$ (1). A solution of Ph_2PCl (11.00 g, 50 mmol) in 50 mL of THF was slowly added to a mixture of $tBuNHNH_2$(HCl) (3.79 g, 30 mmol) and 10.2 g of Et_3N (100 mmol) in 50 mL of THF at ambient conditions. The mixture was stirred for 24 h and then filtered. THF was distilled off, and a large amount of *n*-hexane (~100 mL) was added. Another portion of Et_3N(HCl) was filtered off. The remaining solution was concentrated and left overnight at room temperature. Large colorless crystals of **1** were formed, isolated by filtration and dried in vacuum. Yield: 11.37 g (83%). Anal. Calcd for $C_{28}H_{30}N_2P_2$, %: C, 73.67; H, 6.62; P, 13.57. Found, %: C, 73.59; H, 6.68; P, 13.63. ^{1}H NMR (d_8-toluene, 295 K) δ (ppm): 8.0–6.7 (m, 21H, Ph and NH); 0.76 (s, 9H, *t*Bu). $^{31}P\{^1H\}$ NMR, δ (ppm): 72.6. IR (KBr pellet), ν/cm^{-1}: 3422 (NH), 3053m, 2967m, 1477s, 1433s, 1386w, 1361w, 1304w, 1261m, 1203m, 1094s, 1025m, 880s, 794s, 740s, 720s, 694vs, 643m, 558m, 512m, 476m.

[Co{HN(PPh$_2$)$_2$-κ^2P,P′}$_2$(μ-PPh$_2$)]$_2$ (2). A solution of *t*BuN(H)-N(PPh$_2$)$_2$ (0.27 g, 0.60 mmol) in 10 mL of toluene was added to a solution of cobalt silylamide (0.15 g, 0.40 mmol) in the same solvent (10 mL). The mixture was kept for 48 h at room temperature. Toluene was removed in vacuum and replaced by THF. The mixture was kept overnight at 0 °C. Red-brown crystals of **2** were formed, isolated by filtration and dried in vacuum. Yield: 0.19 g (0.14 mmol, 68%). Anal. Calcd for $C_{80}H_{78}Co_2N_2O_2P_6$ (two THF solvate molecules), %: C, 68.48; H, 5.60; Co, 8.40 Found, %: C, 68.27; H, 5.72; Co, 8.32. ^{1}H NMR (THF- d_8, 295 K) δ (ppm): 3.95 (s, 2H, NH), 6.5–9.5 (m, 60H, Ph). $^{31}P\{^1H\}$ NMR, δ (ppm): 112.2 (m, Ph_2PCo), 22.0 (m, Ph_2PN). IR (nujol), ν/cm^{-1}: 3450w, 1307w, 1091m, 1025w, 973w, 842m, 735s, 695s, 610m, 554w, 532m. UV/vis spectrum (THF): λ_{max} 435 (240), 515 (110) nm.

[Li{Ph$_2$P(NPPh$_2$)$_2$-κ^2N,N′}(THF)$_2$] (4). A solution of $LiN(SiMe_3)_2$ (0.20 g, 1.2 mmol) in 10 mL of toluene was added to a solution of $(Ph_2P)_2N-NH-PPh_2$ (**3**) (0.71 g, 1.2 mmol) in the same solvent (10 mL) at 0 °C. The color of the solution turned yellow. After the mixture was concentrated to 10 mL, 0.5 mL of THF was charged into the system via a syringe, and the crystallization was initiated. The mixture was left undisturbed overnight at 0 °C. Large colorless crystals of **4** were formed, isolated by filtration and dried in vacuum. Yield: 0.68 g (78%). Anal. Calcd for $C_{44}H_{46}LiN_2O_2P_3$, %: C, 71.93; H, 6.31. Found, %: C, 71.85; H, 6.34. ^{1}H NMR (THF-d_8, 295 K) δ (ppm): 7.1–8.1 m (Ph). $^{31}P\{^1H\}$ NMR, δ (ppm): 42.7 (m, $^2J_{A,B}$ = 120 Hz);

dx.doi.org/10.1021/ic201617p | Inorg. Chem. 2012, 51, 874–881

34.1 (m, $^2J_{A,B}$ = 120 Hz). IR (Nujol), ν/cm^{-1}: 1125sh, 1091vs, br, 1062sh, 913m, 897m, 785s, 742s, 727m, 697s, 673m, 542m, 531m, 503m, 474m.

[La{Ph$_2$P(NPPh$_2$)$_2$-κ^2N,N′}{N(SiMe$_3$)$_2$}$_2$ (5). A mixture of **3** (0.29 g, 0.5 mmol) and La[N(SiMe$_3$)$_2$]$_3$ (0.31 g, 0.5 mmol) in toluene (10 mL) was heated at 115 °C for 5 h. The resulting solution was concentrated to 5 and 0.5 mL of Et$_2$O was added. The mixture was left overnight at 0 °C. Colorless crystals of **5** were obtained, isolated by filtration and dried in vacuum. Yield: 0.48 g (92%). Anal. Calcd for $C_{48}H_{66}LaN_4P_3Si_4$, %: C, 55.26; H, 6.38; N, 5.37. Found, %: C, 55.21; H, 6.42; N, 5.33. ^{1}H NMR (THF-d_8, 295 K) δ (ppm): 7.0−8.2 (m, 30H, Ph); −0.51 (s, 36H, Me). ^{31}P{^{1}H} NMR (THF, 295 K), δ (ppm): 41.7 (d, $^2J_{P,P}$ = 36 Hz); 34.2, (t, $^2J_{P,P}$ = 36 Hz). IR (Nujol), ν/cm^{-1}: 1242vs, 1180m, 1110s, 1070w, 980vs, br, 880w, 826s, 806s, 768m, 738m, 714m, 696m, 675m, 592s, 5322s, 506m, 479m.

■ ASSOCIATED CONTENT

Ⓢ Supporting Information

Crystallographic information for **1**, **2**, **4**, and **5** in CIF format; optimized structure of **2** at the B3LYP/6-31G(d) level and selected bond distances and angles; molecular orbitals for **2**, contour maps for the HOMO, HOMO−1 and HOMO−7 and electron density map of **2**; ^{31}P{^{1}H} NMR spectra of **4** and **5**; selected Mulliken charges for **3** and related particles; B3LYP total energy for isomeric ligands; interaction of **1** with MeLi and *n*-BuLi. This material is available free of charge via the Internet at http://pubs.acs.org.

■ AUTHOR INFORMATION

Corresponding Author

*E-mail: akornev@iomc.ras.ru. Fax: +7 (831) 4627497. Phone: +7 (831) 4627795.

■ ACKNOWLEDGMENTS

This work was supported by The Russian President's program "Leading Scientific Schools" (No. 7065.2010.3), State Contracts No. 16.740.11.0015 and No. P-337, and by The Deutsche Forschungsgemeinschaft (HE 1376/29-1). We thank Dr. O. V. Kouznetsova and N. M. Khamaletdinova for IR measurements.

■ REFERENCES

(1) Sakakura, T.; Sodeyama, T.; Sasaki, K.; Wada, K.; Tanaka, M. *J. Am. Chem. Soc.* **1990**, *112*, 7221andreferencs therein.
(2) MacDougall, J. K.; Simpson, M. C.; Green, M. J.; Cole-Hamilton, D. J. *J. Chem. Soc., Dalton Trans.* **1996**, 1161and references therein.
(3) (a) Littke, A. F.; Fu, G. C. *J. Org. Chem.* **1999**, *64*, 10. (b) Littke, A. F.; Fu, G. C. *Angew. Chem,. Int. Ed.* **1999**, *38*, 2411. (c) Wolfe, J. P.; Singer, R. A.; Yang, B. H.; Buchwald, S. L. *J. Am. Chem. Soc.* **1999**, *121*, 9550. (d) Hamann, B. C.; Hartwig, J. F. *J. Am. Chem. Soc.* **1998**, *120*, 7370.
(4) Nagashima, H.; Sue, T.; Oda, T.; Kanemitsu, A.; Matsumoto, T.; Motoyama, Y.; Sunada, Y. *Organometallics* **2006**, *25*, 1987−1994.
(5) Zubiri, M. R. I; Woollins, J. D. *Comments Inorg. Chem.* **2003**, *24*, 189−252.
(6) Ly, T. Q.; Woollins, J. D. *Coord. Chem. Rev.* **1998**, *176*, 451−481.
(7) Ellerman, J.; Sutter, J.; Schelle, C.; Knoch, F. A.; Moll, M. *Z. Anorg. Allg. Chem.* **1993**, *619*, 2006−2014.
(8) Ellermann, J.; Sutter, J.; Knoch, F. A.; Moll, M. *Angew. Chem., Int. Ed.* **1993**, *3*, 700−701.
(9) Ellermann, J.; Schutz, M.; Heinemann, F. W.; Moll, M.; Bauer, W. *Z. Naturforsch., B: Chem. Sci.* **1997**, *52b*, 795−800.
(10) Fedotova, Y. V.; Kornev, A. N.; Sushev, V. V.; Kursky, Yu. A.; Mushtina, T. G.; Makarenko, N. P.; Fukin, G. K.; Abakumov, G. A.; Zakharov, L. N.; Rheingold, A. L. *J. Organomet. Chem.* **2004**, *689*, 3060−3074.
(11) Sushev, V. V.; Kornev, A. N.; Min'ko, Y. A.; Belina, N. V.; Kurskiy, Yu. A.; Kuznetsova, O. V.; Fukin, G. K.; Baranov, E. V.; Cherkasov, V. K.; Abakumov, G. A. *J. Organomet. Chem.* **2006**, *691*, 879−889.
(12) Sushev, V. V.; Belina, N. V.; Fukin, G. K.; Kurskiy, Yu. A.; Kornev, A. N.; Abakumov, G. A. *Inorg. Chem.* **2008**, *47*, 2608−2612.
(13) Kornev, A. N.; Belina, N. V.; Sushev, V. V.; Fukin, G. K.; Baranov, E. V.; Kurskiy, Y. A.; Poddelskii, A. I.; Abakumov, G. A.; Lönnecke, P.; Hey-Hawkins, E. *Inorg. Chem.* **2009**, *48*, 5574−5583.
(14) Belina, N. V.; Kornev, A. N.; Sushev, V. V.; Fukin, G. K.; Baranov, E. V.; Abakumov, G. A. *J. Organomet. Chem.* **2010**, *695*, 637−641.
(15) Kornev, A. N.; Belina, N. V.; Sushev, V. V.; Panova, J. S.; Lukoyanova, O. V.; Ketkov, S. Yu.; Fukin, G. K.; Lopatin, M. A.; Abakumov, G. A. *Inorg. Chem.* **2010**, *49*, 9677−9682.
(16) Bhatacharya, A. K.; Thyagarman, O. *Chem. Rev.* **1981**, *81*, 415−430.
(17) Brill, T. E.; Landon, S. J. *Chem. Rev.* **1984**, *84*, 577−585.
(18) Naumov, V. A.; Vilkov, L. V. *Molecular structures of organophosphorus compounds* (in Russian); Nauka: Moscow, 1986.
(19) Fei, Z.; Dyson, P. J. *Coord. Chem. Rev.* **2005**, *249*, 2056−2074.
(20) Keat, R.; Manojlovid-Muir, L.; Muir, K. W.; Rycroft, D. S. *J. Chem. Soc., Dalton Trans.* **1981**, 2192−2198.
(21) Simon-Manso, E.; Valderrama, M.; Gantzel, P.; Kubiak, C. P. *J. Organomet. Chem.* **2002**, *651*, 90−97.
(22) Cordero, B.; Gomez, V.; Platero-Prats, A. E.; Reves, M.; Echeverria, J.; Cremades, E.; Barragan, F.; Alvarez, S. *Dalton Trans.* **2008**, 2832−2838.
(23) (a) Harley, A. D.; Whittle, R. R.; Geoffroy, G. L. *Organometallics* **1983**, *2*, 383−387. (b) Harley, A. D.; Whittle, R. R.; Geoffroy, G. L. *Organometallics* **1986**, *5*, 1283.
(24) Coleman, J. M.; Dahl, L. F. *J. Am. Chem. Soc.* **1967**, *89*, 542−552.
(25) Harley, A. D.; Whittle, R. R.; Geoffroy, G. L. *Organometallics* **1983**, *2*, 60−63.
(26) Bader, R. F. W. *Atoms in Molecules: A Quantum Theory*; Oxford University Press: Oxford, 1990.
(27) Bradley, D. C.; Hursthouse, M. B.; Smallwood, R. J.; Welch, A. J. *J. Chem. Soc., Chem. Commun.* **1972**, 872.
(28) Putzer, M. A.; Neumuller, B.; Dehnicke, K.; Magull, J. *Chem. Ber.* **1996**, *129*, 715.
(29) Perrin, D. D.; Armarego, W. L. F.; Perrin, D. R. *Purification of Laboratory Chemicals*; Pergamon: Oxford, 1980.
(30) Andersen, R. A.; Faegri, K.; Green, J. C.; Haaland, A.; Lappert, M. F.; Leung, W.-P.; Rypdal, K. *Inorg. Chem.* **1988**, *27*, 1782.
(31) Burger, H.; Wannagat, U. *Monatsh. Chem.* **1963**, *94*, 1007.
(32) Bradley, D. C.; Ghotra, J. S.; Hart, F. A. *Dalton Trans.* **1973**, 1021−1023.
(33) Upor, E.; Mohai, M.; Novak, Gy. *Photometric methods in inorganic trace analysis*; Academiai Kiado: Budapest, 1985.
(34) Sheldrick, G. M. *Acta Crystallogr.* **2008**, *A64*, 112−122.
(35) SCALE3 ABSPACK: CrysAlisPro, Agilent Technologies, Version 1.171.34.44. Empirical absorption correction using spherical harmonics, implemented in SCALE3 ABSPACK scaling algorithm.
(36) Sheldrick, G. M. SADABS v.2.01, *Bruker/Siemens Area Detector Absorption Correction Program*; Bruker AXS: Madison, WI, USA, 1998.
(37) Carpenter, J. E.; Weinhold, F. J. *Mol. Struct. (THEOCHEM)* **1988**, *169*, 41−62.
(38) Keith, T. A. *AIMAll (Version 10.12.08)*; 2010 (aim.tkgristmill.com).